Exposure Concentration Prediction by Multi-Nesting Approach Connecting Building Space-Virtual Manikin-Nasal Airway Model

Kazuhide Ito* and Hiroaki Asanuma

IGSES, Kyushu University
6-1 Kasuga-koen, Kasuga
Fukuoka, Japan

**Corresponding author: ito@kyudai.jp*

ABSTRACT
In this study, we developed an integrated simulation procedure for prediction of concentration of contaminant exposure using a multi-nesting method connecting building space, a Virtual Manikin, and bronchus airway in humans. On the basis of this numerical simulation, detailed information on the unsteady spacial distribution of contaminant concentration, the breathing concentration of infectious contaminant, and the non-uniform distribution of contaminant deposition in nasal airway could be provided for designers of indoor environments in the design stage and also for residents. Here, we demonstrate the application of this integrated multi-nesting approach for targeting a waiting space in a university hospital.

KEYWORDS
Airway, Virtual Manikin, CFD, Nesting, Infectious Transmission

INTRODUCTION

Indoor environmental issues, especially air-quality problems, are being addressed more and more intensively, and this trend looks set to continue. From the viewpoint of management of public health for residents or workers, the prediction and control of the concentration of contaminant in occupational exposure will be critically important for the production of healthy indoor environments. In general, concerning problems of low-concentration and long-term exposure, for example, exposure to formaldehyde and volatile organic compounds (VOCs) emitted from building materials, time- and space-averaged concentration in a whole room or occupied zone will be the controlled target of air-quality management; the necessity of evaluating and predicting time fluctuations and distributions of contaminant on a short time scale is low. On the other hand, concerning the problems of high-concentration and short-term exposure by terorrism involving nuclear, biological, and chemical weapons (NBC), gas leak accidents, and/or imperfect combustion of waste gas from burning appliances, with a local or point concentration, the breathing concentration of contaminant will present a mortal danger. More specifically, the unsteady and non-uniform concentration distribution of a target contaminant becomes a critical parameter of residential air-quality management.
In this paper, we propose a method for prediction of residential exposure concentration level from building scale to nasal airway scale inside of the human body. Here, an integrated numerical procedure of CFD technique, that is, a multi-nesting method, is applied to infectious transmission in a hospital space caused by a hypothetical acute respiratory contaminant.

OUTLINE OF TARGET SPACE AND GRID DESIGN

University Hospital (Region 1)

In this study, the waiting space of a university hospital as Region 1 is analyzed. Figure 1 shows the outline of the hospital space and the plan of the first floor, which is 42 m × 90 m and with a total floor area of 2020 m^2. This region consists of three zones: (i) reception and waiting space on the north side (3.0 m in height), (ii) hospital mall on the south side (15 m in height), and (iii) medical space on the west side; there is a heating, ventilation, and air-conditioning (HVAC) system designed and constructed in accordance with these three zones. The numerical analysis was conducted in zones (i) and (ii) because the doors of the rooms in zone (iii) are always closed and its HVAC system is also independent. Multiple fan coil units (FCU) are arranged in zones (i) and (ii) in order to control the indoor temperature. A total of 79 supply inlet openings of the air-conditioning system are installed on the ceiling and air is exhausted through lavatories in three places. The geometries of the hospital space, furniture, and the supply inlet and exhaust outlet openings were simplistically modeled in order to avoid them having predominant effects on the prediction accuracy.

This space (Region 1) was discretized by an unstructured mesh and the total number of meshes was set to approximately 600,000 for the analysis.

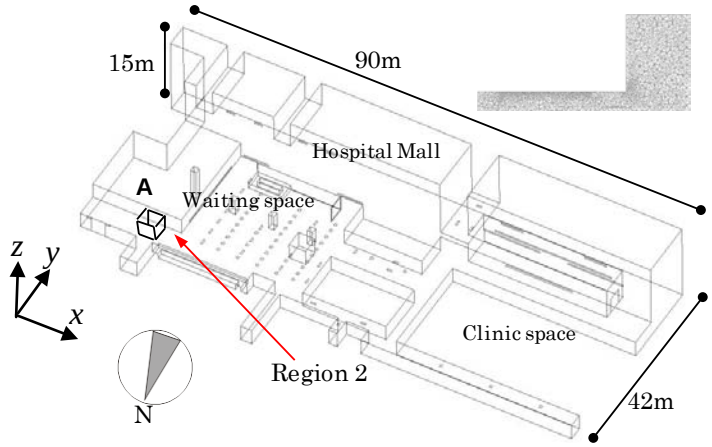

Figure 1 Perspective View of University Hospital (Region 1)

Virtual Manikin (Region 2)

Indoor environmental studies have focused on physical phenomena around the human body at the microclimate level in recent years; therefore, the need for realistic and detailed human body models, for example, Virtual Manikin or Computer Simulated Person, has been pointed out. In this study, a Virtual Manikin that reflected the average Japanese body proportions (standing adult male) was developed.

The outlines of the human body were drawn using POSER 4.0J software (Curious Labs Inc.) and the data were then read out in DXF format. The overall shape of the human body was then adjusted using three-dimensional CAD software (Vector Works and A&A Co. Ltd.). The final geometry of the Virtual Manikin and computational grids were made using GRIDGEN V15 (VINAS Co. Ltd.). The hands and feet of the Virtual Manikin were simplified in consideration of the computational load for the CFD analysis.

The Virtual Manikin was arranged at the northeast corner and in front of the lavatory in Region 1 and an analytical domain of dimensions x=3.0 m, y=3.0 m, and z=3.0 m was set by centering on a standing Virtual Manikin (see point A in Figure 1). Figure 2 denotes the outline of Region 2. The ceiling height of Region 2 corresponds to that of Region 1 and there is no supply and exhaust opening of the air-conditioning system.

The total number of computational cells in Region 2 was set to about 1.02 million. The surface mesh reproduced the complex geometry of the human body arranged with a triangular

surface mesh. To resolve the boundary layer around the Virtual Manikin, four layers of prism cells were created on its surface with an equal height of 1.0 mm between layers. The tetra-meshes were then arranged from the outside of the boundary layer to the other side walls in the analytical model room. Under this numerical condition, the wall units (y^+), which express the dimensionless normal distance from the surface, met the requirement of 1.0 or less over the whole surface of the Virtual Manikin.

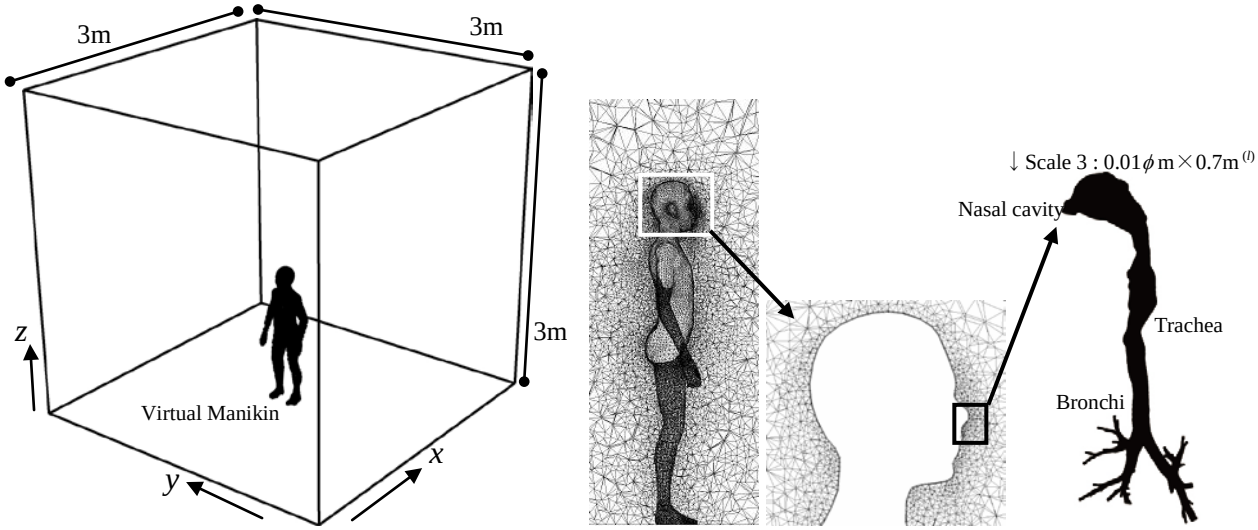

Figure 2 Perspective View of Virtual Manikin (Region 2) and Airway Model (Region 3)

Nasal Airway Inside Human Body (Region 3)

Airway model from nasal cavity to bronchial tubes (fourth bifurcation) was arranged as Region 3 and nasal cavity (nostril) was set as the boundary with Region 2. A computational airway model was created using computed tomography (CT) data (DICOM format) of a healthy adult male (average height and weight of Japanese). The smoothing of the overall shape and the creation of fluid geometries were adjusted by Mimics 4.0 (Materialise) and 3-matic (Materialise) software. The final geometry of the airway model and computational grids were made using GRIDGEN V15 (VINAS).

The total number of computational cells in Region 3 was set to about 1.0 million and the wall units (y^+) met the requirement of 1.0 or less over the whole surface of the airway model.

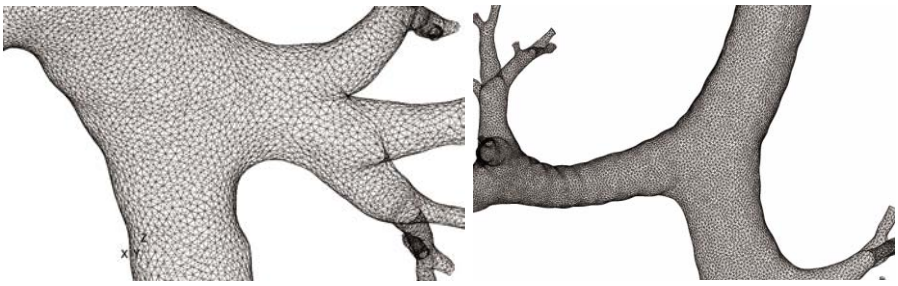
Figure 3 Detailed Grid Design of Airway Model

OUTLINE OF NUMERICAL SIMULATION

In order to connect three different analytical domains (Regions 1, 2, and 3), a one-way nesting method was applied in this analysis. From Region 1 to Region 2, distributions of average velocities (U, V, and W), turbulent properties (k and ε), and unsteady contaminant concentration distribution data were transferred. Each piece of data that passed from Region 1 to Region 2 was linearly interpolated because the size of the grid was markedly different on the boundary plane in the two regions.

From Region 2 and Region 3, the flow field in the vicinity of the nostrils is assumed to be determined almost completely dependently on the respiratory cycle of the human body; hence, the inlet velocity of the boundary plane in Region 2 and Region 3 was calculated from the steady breathing air volume and only contaminant concentration data in the breathing zone were transferred from Region 2 to Region 3.
The purpose of this simulation is to demonstrate the analytical procedure and provide an application example; then, every simulation was conducted under isothermal conditions for the reduction of computational load. The commercial CFD code ANSYS/Fluent 12 (ANSYS Co. Ltd.) was used to calculate the flow field and contaminant distributions.

Region 1
Flow fields were analyzed by the RNG k-ε model in the steady state condition [22]. The SIMPLE algorithm was used with the QUICK scheme for the convective terms, and a second-order center difference scheme was used for the others. After steady flow field analysis, unsteady aerosol contaminant concentration distributions were analyzed by solving ensemble-averaged scalar transport equation based on a Eulerian approach. Contaminant was assumed to be aerosol particles and their diameter was set to 10 μm. The contaminant was assumed to be generated through 16 points of supply inlet openings of the air-conditioning system in the zone (i) reception and waiting space constantly for two hours, and subsequently reached a concentration of zero at supply inlet positions.

Table 1 Numerical and Boundary Conditions of Region 1

Turbulence Model	RNG k-ε model (3-dimensional Cal.)
Scheme	Convection Term: QUICK
Inflow Boundary	U_{in} =0.5 [m/s], k_{in} =3/2× (U_{in}×0.1)^2, ε_{in} =$C_\mu^{3/4}$×$k_{in}^{3/2}$/l_{in}, C_μ=0.09, l_{in} =0.03 [m]
Outflow Boundary	U_{out} = free slip, k_{out}= free slip, ε_{out} = free slip
Wall Treatment	Velocity: generalized log low, Contaminant: gradient zero
Contaminant	D_p=10 μm, Eulerian approach

Region 2
The flow field was analyzed three-dimensionally on the basis of the low Reynolds number k-ε model (Abe-Nagano-Kondo model) in the steady state condition. The SIMPLE algorithm was used with the QUICK scheme for the convective terms, and a second-order center difference scheme was used for the others. The no-slip condition was adopted as the wall surface boundary condition for velocity. After the steady state analysis of flow field around the Virtual Manikin, the analyses of unsteady contaminant concentration distributions were carried out under conditions that considered convection, diffusion, and gravitational sedimentation for Dp= 10-μm-size particle based on a Eulerian approach. Table 2 shows details of the numerical and boundary conditions for Region 2. In this analysis, breathing cycle (inhaled and exhaled air flow) and heat generation from the Virtual Manikin were not reproduced.

Table 2 Numerical and Boundary Conditions of Region 2

Turbulence Model	Low Re Type model (Abe-Nagano model, 3-dimensional Cal.)
Scheme	Convection Term: QUICK
Region 1 and 2 Boundary	U_{in} : Region 1 Data , k_{in}: Region 1 Data, ε_{in}: Region 1 Data
Wall Treatment	Velocity: No-slip, $k\|_{wall}$: no slip, $\varepsilon\|_{wall} = 2\nu(\partial\sqrt{k}/\partial y)^2$, Contaminant: gradient zero
Contaminant	D_p=10 μm, Eulerian approach

Region 3

The flow field was also analyzed on the basis of the low Reynolds number k-ε model (Abe-Nagano-Kondo model) and no-slip condition was adopted as the wall surface boundary condition. Unsteady distribution of aerosol contaminant was analyzed using a Lagrangian model, which analyzes transient momentum equation for each particle and includes drag force and gravitational effect. Discrete random walk model was adopted to model stochastic turbulent dispersion. A total of 10,000 particles, which were assumed to have a spherical shape, were generated from the inlet plane at moment and unsteady particle trajectory was carried out under the perfect sink wall boundary condition.

Table 3 Numerical and Boundary Conditions of Region 3

Turbulence Model	Low Re Type k-ε model (Abe-Nagano model, 3-dimensional Cal.)
Scheme	Convection Term: QUICK
Inflow Boundary	U_{in}=0.92 [m/s], k_{in}=3/2× (U_{in}×0.1)^2, $\varepsilon_{in}=C_\mu^{3/4}\times k_{in}^{3/2}/l_{in}$, C_μ=0.09, $l_{in}=10^{-3}$[m]
Outflow Boundary	U_{out} = free slip, k_{out}= free slip, ε_{out} = free slip
Wall Treatment	Velocity: No-slip, $k\|_{wall}$: no slip, $\varepsilon\|_{wall}=2\nu(\partial\sqrt{k}/\partial y)^2$, Contaminant: perfect sink
Contaminant	D_p=10 μm, Lagrangian approach

RESULTS

Region 1

The results of flow field and contaminant concentration distribution in Region 1 are shown in Figure 4. Stagnant flow field was formed except for in the vicinity of the supply inlet opening and lavatory space, which was designed as an exhaust outlet. As for the contaminant distribution, aerosol contaminant was distributed within the zone (i) waiting space of the hospital in accordance with the zoning of the air-conditioning system and contaminant generation points.

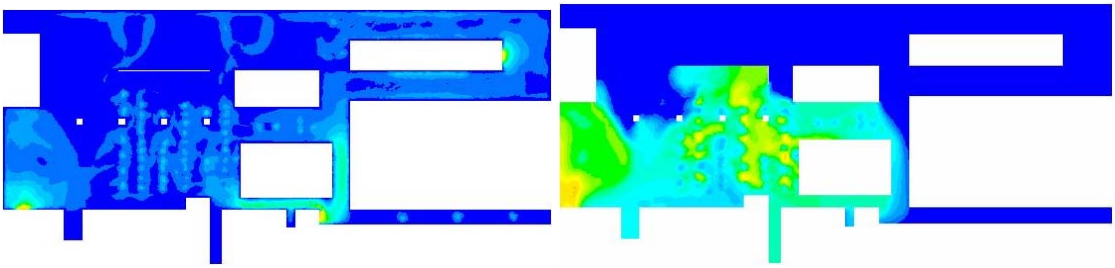

(1) Flow fluid (y=1.6 m, m/s) (2) Contaminant distribution (t=2 hours)

Figure 4 Results of Flow Field and Contaminant Distribution in Hospital (Region 1)

The flow field in the nesting region from Region 1 to Region 2 (see point **A** in Figure 1) is shown in Figure 5(1); a stagnant flow field with air velocity below 0.15 m/s and flow from the center of the waiting space to the lavatory space was formed. Figure 5(2) denotes the concentration distribution of D_p= 10-μm-size aerosol contaminant in the same nesting region.

Region 2

The Virtual Manikin faced the east side of the hospital building.

Figure 5(3) indicates the concentration distribution of the aerosol contaminant in Region 2 with the Virtual Manikin. This is the result from two hours after the start of analysis, and the concentration in Figure 5(3) was normalized by the supply inlet concentration of the air-conditioning system on the ceiling. The existence of the Virtual Manikin influenced the flow field and contaminant distribution in Region 2.

In Figure 6, the estimation results of time histories of breathing concentration and total inhalation dose of the Virtual Manikin are shown. Here, the pulmonary ventilation rate of the Virtual Manikin was assumed to be 1.67×10^{-4} [m^3/s] for estimation of total inhalation dose.

Air change rate of Region 1 was 4.36 [h^{-1}] and hence contaminant concentration in the breathing zone reached a steady state from the beginning of contaminant generation within tens of minutes as shown in Figure 6(1). The breathing concentration immediately decreased after the cessation of contaminant generation (t=2 hours).

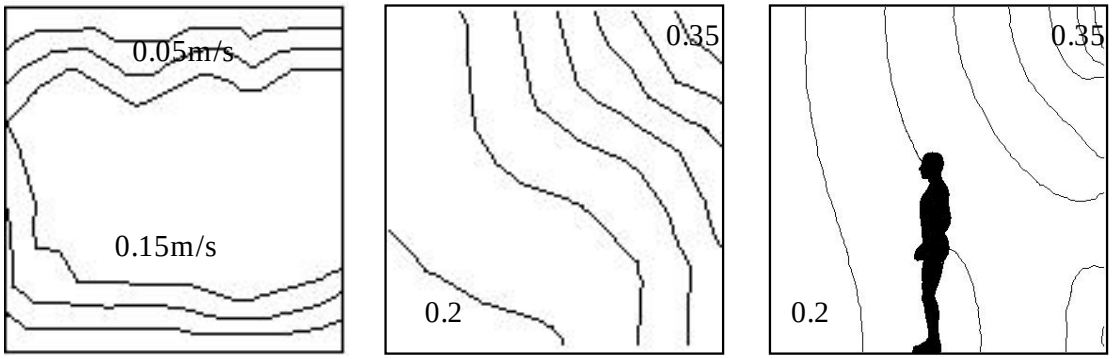

(1) Flow field (without Virtual Manikin) (2) Concentration distribution (without Virtual Manikin) (3) Concentration distribution (with Virtual Manikin)

Figure 5 Flow Field and Contaminant Distribution in Region 2

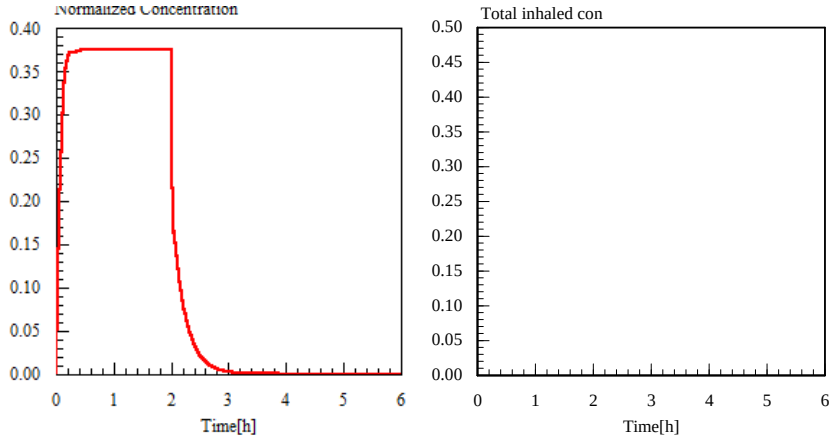

(1) Breathing concentration (2) Total inhalation dose

Figure 6 Results of Time Series of Exposure Concentration (Region 2)

Region 3

The results of flow field and path line of aerosol particles are shown in Figure 7. The results of relatively large particles (Dp= 50 μm) as well as fine particles (Dp= 10 μm) are introduced for reference.

The flow inside the airway model was analyzed under the hypothesis of constant inhalation and steady state. A complicated flow field was formed in the airway model because of the complex geometry. Concerning the 10-μm-size particles, 66% of total generated particles at the boundary of the nares were deposited on the surface of the nasal cavity and the rest were transported until the third bifurcation of bronchial tubes through the pharyngis. On the other hand, 100% of the 50-μm-size particles were deposited at the inner wall of the nasal cavity and were not transported as far as the bronchus.

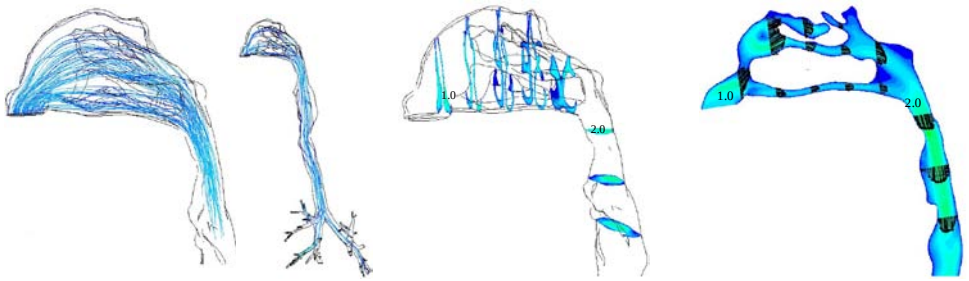

(1) Stream line (2) Velocity maginitude (m/s) (3) Velocity vector (m/s)

(4) Path line of Dp= 10 μm particles (5) Path line of Dp= 50 μm particles

Figure 7 Results of Stream Line and Path Line of Contaminant (Region 3)

DISCUSSION

A previous research paper reported that particles of micrometer order or above were deposited and captured in the upper airway region and particles of the order of 0.1 μm or below reached deep into the lungs. Our simulation results show the possibility of 10-μm-size particles passing through the nasal airway. However, the reproducibility of flow and contaminant distribution in the airway model will be strongly dependent on the degree of roughness of the surface geometry. Fluid resistance of nasal hair and interaction between particles in air phase and the surface of the airway model, and also the respiration cycle, will also be important factors to improve prediction accuracy.

Here, we proposed an integrated simulation procedure for prediction of concentration of contaminant exposure using a multi-nesting method connecting building space, a Virtual Manikin, and bronchus airway in humans and showed an application example of this procedure. The nesting from Region 2 to Region 3 was insufficient in this study and the development of a seamless nesting method to connect breathing information of the Virtual Manikin and the boundary of nasal airway is an important research issue for the future.

CONCLUSION

A comprehensive numerical prediction based on one-way nesting method that directly connects the boudary conditions from hospital building scale to nasal airway inside a human by the intermediate of a Virtual Manikin was proposed in this study.

The findings obtained in this work can be summarized as follows:

(1) One-way downscaling analysis of residential exposure concentration for a large-scale hospital waiting space was demonstrated. The possibility of an engineering approach was represented for the estimation of breathing contaminant concentration and non-uniform distribution of aerosol deposition inside nasal airway.

(2) In the future, the experimental validation and improvement of prediction accuracy of this proposed numerical procedure will be needed.

ACKNOWLEDGEMENTS

This research was partly supported by a Grant-in-Aid for Scientific Research (JSPS KAKENHI for Young Scientists (S), 21676005). The authors would like to express special thanks to the funding source.

REFERENCES

[1] Ma, B. and Lutchen, K.R., CFD simulation of aerosol in an anatomically based human large-medium airway model, Annals of Biomedical Engineering, Vol.37, No.2, 2009, pp.271-285

[2] Longest, P.W. and Vinchurkar, S., Validating CFD predictions of respiratory aerosol deposition: Effects of upstream transition and turbulence, Journal of Biomechanics, 40, 2007, pp305-316

[3] Deschamps, T., Schwartz, P., Trebotich, D., Air-flow simulation in realistic models of the trachea, Proceedings of the 26th Annual International Conference of the IEEE EMBS, 2004, pp3933-3936

[4] Stapleton, K.W., Guentsch, E., Hoskinson, M.K., Finlay, W.H., On the suitability of k-ε turbulence modeling for aerosol deposition in the mouth and throat: A comparison with experiment, Journal of Aerosol Science 31 (6), 2000, pp739-749

[5] .Schroeter, J.D., Garcia, G.J.M., Kimbell, J.S., 2011. Effects of surface smoothness on inertial particle deposition in human nasal models, Journal Aerosol Science 42, 2011, pp52-63

[6] Asanuma, A., and Ito, K., Integrated Approach of CFD and SIR Epidemiological Model for Infectious Transmission Analysis in Hospital, AIVC 2011 conference proceedings (submitted)